The δ2 glutamate receptor gates long-term depression by coordinating interactions between two AMPA receptor phosphorylation sites

Kazuhisa Kohda[a,b,1], Wataru Kakegawa[a,b,1], Shinji Matsuda[a,b,c], Tadashi Yamamoto[d], Hisashi Hirano[e], and Michisuke Yuzaki[a,b,2]

[a]Department of Physiology, School of Medicine, Keio University, Shinjuku-ku, Tokyo 160-8582, Japan; [b]Core Research for Evolutional Science and Technology (CREST) and [c]Precursory Research for Embryonic Science and Technology (PREST), Japan Science and Technology Agency, Kawaguchi, Saitama 332-0012, Japan; [d]Cell Signal Unit, Okinawa Institute of Science and Technology Graduate University, Kunigami, Okinawa 904-0495, Japan; and [e]Division of Functional Proteomics, Yokohama City University, Turumi-ku, Yokohama 230-0045, Japan

Edited* by Masao Ito, RIKEN Brain Science Institute, Wako, Japan, and approved January 24, 2013 (received for review October 23, 2012)

Long-term depression (LTD) commonly affects learning and memory in various brain regions. Although cerebellar LTD absolutely requires the δ2 glutamate receptor (GluD2) that is expressed in Purkinje cells, LTD in other brain regions does not; why and how cerebellar LTD is regulated by GluD2 remains unelucidated. Here, we show that the activity-dependent phosphorylation of serine 880 (S880) in GluA2 AMPA receptor subunit, which is an essential step for AMPA receptor endocytosis during LTD induction, was impaired in *GluD2*-null cerebellum. In contrast, the basal phosphorylation levels of tyrosine 876 (Y876) in GluA2 were increased in *GluD2*-null cerebellum. An in vitro phosphorylation assay revealed that Y876 phosphorylation inhibited subsequent S880 phosphorylation. Conversely, Y876 dephosphorylation was sufficient to restore S880 phosphorylation and LTD induction in *GluD2*-null Purkinje cells. Furthermore, megakaryocyte protein tyrosine phosphatase (PTPMEG), which binds to the C terminus of GluD2, directly dephosphorylated Y876. These data indicate that GluD2 gates LTD by coordinating interactions between the two phosphorylation sites of the GluA2.

synaptic plasticity | mouse

Synaptic plasticity, such as long-term potentiation and long-term depression (LTD), is believed to underlie learning and memory processes in vivo. LTD is observed in various brain regions, including the cerebellum and hippocampus, and it is commonly caused by clathrin-dependent endocytosis of postsynaptic AMPA-type glutamate receptors. However, cerebellar LTD is unique, because it requires the presence of another class of glutamate receptors, the δ2 glutamate receptor (GluD2) (1), which is predominantly expressed in parallel fiber (PF)–Purkinje cell synapses. *GluD2*-null mice display ataxia and impaired motor learning (2). GluD2 does not normally function as an ion channel; instead, its C-terminal end, which constitutes a postsynaptic density-95/discs-large/zonula occludens-1 (PDZ) ligand domain, is essential for LTD induction. LTD is abolished in WT Purkinje cells that have been acutely perfused with a short peptide that corresponds to the PDZ ligand domain of GluD2 (3). Although morphological abnormalities in *GluD2*-null cerebellum are rescued by the expression of a mutant GluD2 transgene that lacks the PDZ ligand domain, LTD and motor learning remain impaired (4). These results indicate that the C terminus of GluD2, to which several PDZ proteins, such as PSD-93, megakaryocyte protein tyrosine phosphatase (PTPMEG), S-SCAM, n-PIST, and delphilin, bind (5), plays a crucial role in LTD induction and motor learning. However, an answer to the fundamental question of how GluD2 regulates cerebellar LTD remains unelucidated.

AMPA receptor endocytosis is generally regulated by changes in the phosphorylation status of AMPA receptor subunits. The activity-dependent phosphorylation of serine 880 (S880) in the GluA2 subunit plays an important role in AMPA receptor endocytosis and LTD induction through the release of glutamate receptor interacting protein 1, which is an anchoring protein, from the C terminus of the AMPA receptors at both hippocampal (6, 7) and cerebellar synapses (8–10). However, how this process is regulated and how it mediates LTD is not completely understood. In addition to the phosphorylation of S880, the phosphorylation of tyrosine 876 (Y876) in the GluA2 subunit regulates AMPA receptor endocytosis during metabotropic glutamate receptor (mGluR) -dependent LTD at hippocampal synapses (11–14). However, whether Y876 phosphorylation is involved in cerebellar LTD, which is dependent on mGluR1, is unknown. In addition, its relationship with S880 phosphorylation is unclear.

In this study, we show that the activity-dependent phosphorylation of S880 in GluA2 was impaired in *GluD2*-null cerebellum. In contrast, the basal phosphorylation levels of Y876 in GluA2 were increased in *GluD2*-null cerebellum. Y876 phosphorylation inhibited subsequent S880 phosphorylation. Conversely, Y876 dephosphorylation restored S880 phosphorylation and LTD induction in *GluD2*-null Purkinje cells. Furthermore, interactions with the tyrosine phosphatase PTPMEG (15) at the C terminus of GluD2 were necessary and sufficient for GluD2 to regulate LTD induction. These results indicated that GluD2 serves as a master switch to gate inducibility of LTD by coordinating interactions between the two phosphorylation sites in GluA2 through its interaction with PTPMEG. Because PTPMEG and GluD1, which is a protein in the GluD2 family, are expressed in regions outside the cerebellum, similar regula-

Significance

Long-term depression (LTD) commonly affects learning and memory in various brain regions. Although LTD in the cerebellum absolutely requires δ2 glutamate receptors, its underlying mechanisms remain elusive. LTD is caused by endocytosis of AMPA receptors, which is triggered by activity-induced serine phosphorylation of the GluA2 subunit. Our work showed that this serine phosphorylation required prior dephosphorylation of the nearby tyrosine residue. By interaction with a tyrosine phosphatase, δ2 glutamate receptors regulated tyrosine dephosphorylation status of GluA2 to gate inducibility of LTD. These findings will provide better understanding of general mechanisms regulating AMPA receptor endocytosis during synaptic plasticity.

Author contributions: K.K., W.K., and M.Y. designed research; K.K. and W.K. performed research; S.M., T.Y., and H.H. contributed new reagents/analytic tools; K.K. and W.K. analyzed data; and K.K. and M.Y. wrote the paper.

The authors declare no conflict of interest.

*This Direct Submission article had a prearranged editor.

[1]K.K. and W.K. contributed equally to this work.

[2]To whom correspondence should be addressed. E-mail: myuzaki@a5.keio.jp.

This article contains supporting information online at www.pnas.org/lookup/suppl/doi:10.1073/pnas.1218380110/-/DCSupplemental.

tory mechanisms of AMPA receptor endocytosis may be operational in other brain regions.

Results

Increased Basal Phosphorylation Levels of Tyrosine in *GluD2*-Null Purkinje Cells. The phosphorylation of S880 (6–10) or Y876 (11, 12, 14, 16) in GluA2 (Fig. 1*A*) has been proposed to play important roles in AMPA receptor endocytosis and LTD. Thus, we first examined the basal phosphorylation of GluA2 in the synaptosomal fraction of cerebellar tissue from postnatal days (P) 21–30 WT and *GluD2*-null mice. An immunoblot analysis with phosphorylation-specific antibodies revealed weak basal phosphorylation of S880 and Y876 in GluA2 in WT cerebellum (Fig. 1*B* and Fig. S8). Basal phosphorylation levels of S880 in GluA2 were similar in WT and *GluD2*-null cerebellum (0.77 ± 0.19-fold vs. WT, $n = 7$ each, $P = 0.15$). Basal phosphorylation levels of Y876 in GluA2 were significantly increased in *GluD2*-null cerebellum compared with those levels in WT cerebellum (1.29 ± 0.11-fold vs. WT, $n = 11$ each, $P = 0.02$) (Fig. 1*B*). Thus, the loss of GluD2 from PF–Purkinje cell synapses increased the tyrosine phosphorylation levels of GluA2 in the cerebellum.

To clarify whether the increased phosphorylation levels of Y876 in GluA2 that were observed in the immunoblot analyses (Fig. 1*B*) reflected changes in the PF synapses of Purkinje cells, we examined PF-evoked slow excitatory postsynaptic currents ($_{slow}$EPSCs), which are activated by mGluR1 and regulated by the tyrosine phosphorylation levels of Purkinje cells (Fig. 1*A*) (17). We performed patch-clamp recordings in acutely prepared slices from P21–P35 mice and adjusted the PF stimulus intensity to evoke similar amplitudes of fast EPSCs, which are mediated by AMPA receptors ($_{AMPA}$EPSCs), between WT and *GluD2*-null Purkinje cells. Then, to evoke and isolate $_{slow}$EPSCs, tetanic stimulation (2–10 pulses at 100 Hz) was applied to PFs in the presence of the AMPA receptor antagonist NBQX. We observed that the amplitudes (Fig. 1*C*) and transferred charges of $_{slow}$EPSCs, which were normalized by transferred charges of $_{AMPA}$EPSCs, were significantly smaller in *GluD2*-null cells than those values in WT Purkinje cells (Fig. 1*C*) ($P = 0.001$ for amplitudes and $P = 0.006$ for transferred charges). PF-evoked $_{slow}$EPSCs were activated by mGluR1, which is coupled to the opening of the canonical transient receptor potential channel 1 (TRPC1) or TRPC3 (Fig. 1*A*) (18, 19). However, the immunohistochemical and immunoblot analyses did not show any decreases in the expression levels of mGluR1, TRPC1, or TRPC3 between WT and *GluD2*-null Purkinje cells (Fig. S1). Indeed, the functions of mGluR1 itself have been reported as normal in *GluD2*-null Purkinje cells (20). These data suggested that the phosphorylation levels of tyrosine were increased in *GluD2*-null Purkinje cells.

To further test this hypothesis, we reduced the tyrosine phosphorylation levels in WT and *GluD2*-null Purkinje cells by introducing 4-amino-1-*tert*-butyl-3-(1′-naphthyl)pyrazolo[3,4-d] pyrimidine (a PP1 analog; 10 μM for 20 min), which is a specific Src family tyrosine kinase (SFK) inhibitor, using a patch pipette. As

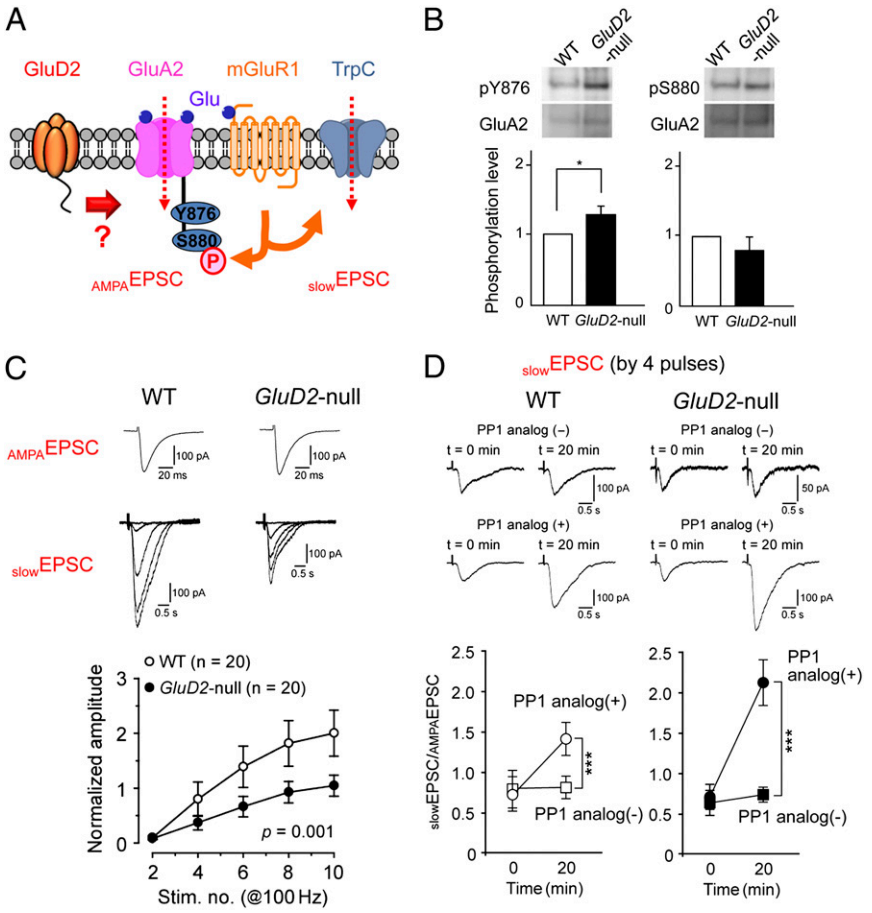

Fig. 1. Increased tyrosine phosphorylation in *GluD2*-null mice. (*A*) A schematic diagram illustrating the positions of Y876 and S880 at the C terminus of GluA2. LTD-inducing stimulation activates the mGluR1 and PKC to phosphorylate S880, which is an essential step for AMPA receptor endocytosis during LTD. mGluR1 activation also induces $_{slow}$EPSCs through the transient receptor potential channel (TRPC). In this paper, we have discussed whether and how GluD2 regulates these processes. (*B*) Basal-state phosphorylation of Y876 and S880 of GluA2 subunits of AMPA receptors in *GluD2*-null mice. Representative immunoblot images of the synaptosomal fraction of WT and *GluD2*-null cerebellum using an antibody against phosphorylated Y876 (pY876) or S880 (pS880) are shown in *Upper*. *Lower* shows intensities of pY876 (*Left*) or pS880 (*Right*) bands in *GluD2*-null cerebellum normalized by intensities of pY876 or pS880 bands in WT cerebellum. Basal-state phosphorylation of Y876, but not S880, was significantly increased in *GluD2*-null cerebellum. The bar represents mean and SEM. *$P < 0.05$ ($n = 11$ for Y876; $n = 7$ for S880). (*C*) Reduced $_{slow}$EPSC amplitudes in *GluD2*-null Purkinje cells. By adjusting PF stimulus intensities, similar sizes of PF-evoked $_{AMPA}$EPSCs were obtained in *GluD2*-null and WT Purkinje cells (*Top*). Then, PFs were stimulated 2–10 times at 100 Hz in the presence of AMPA receptor blockers to evoke $_{slow}$EPSCs (*Middle*). Amplitudes of $_{slow}$EPSCs were normalized by amplitudes of $_{AMPA}$EPSCs and plotted against the number of stimulations in *Bottom*. The bar represents mean and SEM. $P = 0.001$ ($n = 20$ each). (*D*) $_{slow}$EPSC amplitudes are enhanced by an SFK inhibitor PP1 analog in both WT and *GluD2*-null Purkinje cells. PFs were stimulated four times at 100 Hz in the presence of AMPA receptor blockers to evoke $_{slow}$EPSCs. When a PP1 analog was not included in the patch pipette [*Top*; PP1 analog (–)], there were no changes in amplitudes of $_{slow}$EPSCs between 0 and 20 min, whereas when a PP1 analog was included (*Middle*; +), amplitudes of $_{slow}$EPSCs at 20 min were significantly increased in both WT and *GluD2*-null Purkinje cells. *Lower* shows potentiating effects by a PP1 analog on $_{slow}$EPSC amplitudes, which were normalized by amplitudes of $_{AMPA}$EPSCs, in WT and *GluD2*-null Purkinje cells. The bar represents mean and SEM. ***$P < 0.005$ ($n = 11$ for each group).

reported previously (17), $_{slow}$EPSCs that are evoked by a submaximal tetanus stimulus (four pulses at 100 Hz) to PFs significantly increased in response to the intracellular loading of a PP1 analog into WT Purkinje cells (Fig. 1 *C* and *D*). The reduced $_{slow}$EPSC amplitudes in *GluD2*-null Purkinje cells were rescued by treatment with the PP1 analog (Fig. 1 *C* and *D*). The PP1 analog exerted stronger enhancing effects on the $_{slow}$EPSC amplitudes in *GluD2*-null cells than the WT Purkinje cells; this finding may reflect higher basal tyrosine phosphorylation levels in *GluD2*-null Purkinje cells. These results indicated that the phosphorylation levels of tyrosine (including Y876 in GluA2) were generally increased at postsynaptic sites of PF–Purkinje cell synapses in *GluD2*-null cerebellum.

Activity-Dependent Increases in Y876 Phosphorylation Inhibited Activity-Induced S880 Phosphorylation in *GluD2*-Null Purkinje Cells. To biochemically determine the changes in the phosphorylation state of GluA2 during cerebellar LTD, we used a chemical LTD protocol, which involved a combination of 50 mM K^+ and 10 μM L-glutamate (K-glu), to mimic the climbing fiber-evoked depolarization of Purkinje cells and PF-induced activation (21). Cell lysates from WT and *GluD2*-null cerebellar slices that were treated with K-glu for 5 min were subjected to immunoblot analyses with phosphorylation-specific antibodies. We confirmed that S880 phosphorylation had significantly increased with K-glu treatment in WT cerebellum (1.84 ± 0.44-fold vs. no treatment control, $n = 8$ each, $P = 0.04$) (Fig. 2*A*), as reported previously (21). In contrast, K-glu treatment failed to induce S880 phosphorylation in *GluD2*-null cerebellum (1.15 ± 0.16-fold vs. control, $n = 13$ each, $P = 0.56$) (Fig. 2*B*). These data supported the concept that the phosphorylation of S880 in GluA2 was essential for cerebellar LTD (8, 10) and indicated that this step was impaired in *GluD2*-null cerebellum.

Although the rapid dephosphorylation of GluA2 tyrosine (12, 22), particularly at Y876 (14), has been reported in mGluR-dependent LTD in the hippocampus, whether Y876 phosphorylation is involved in cerebellar LTD has been unclear. We found that K-glu treatment significantly decreased the phosphorylation levels of Y876 in WT cerebellum (0.58 ± 0.12-fold vs. control, $n =$

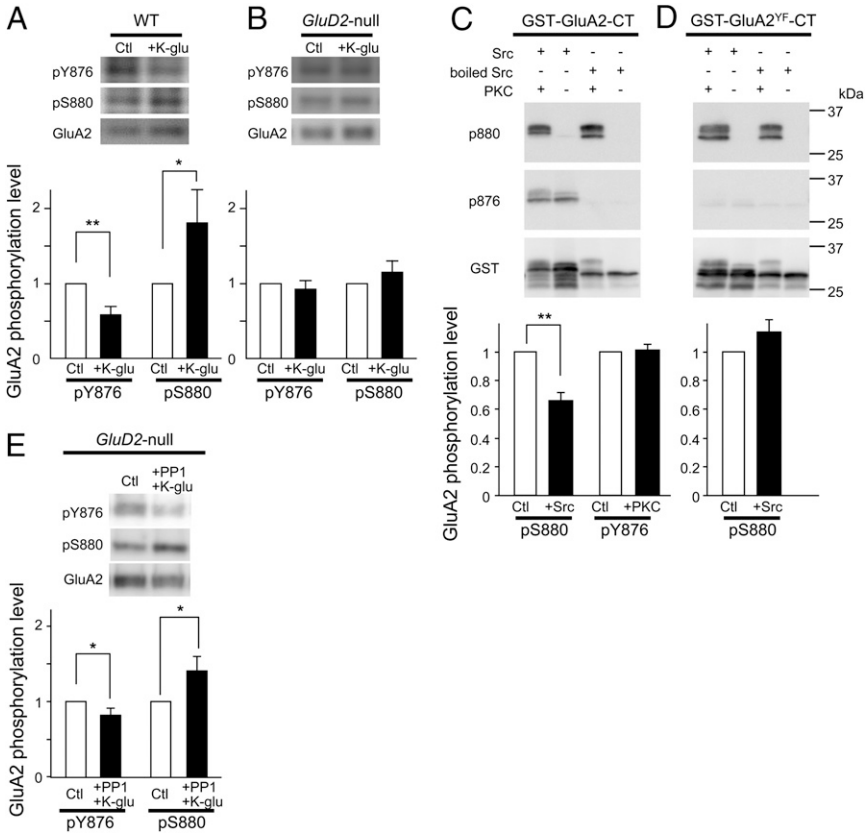

Fig. 2. Increased Y876 phosphorylation inhibits S880 phosphorylation. (*A* and *B*) Chemical LTD stimulus decreases Y876 phosphorylation but increases S880 phosphorylation in WT cerebellum (*A*), whereas it induces no changes at both sites in *GluD2*-null cerebellum (*B*). WT and *GluD2*-null cerebellar slices were treated with 50 mM KCl plus 10 μM L-glutamate for 5 min (K-glu), and the cell lysates were subjected to immunoblot analyses using phosphorylation-specific antibodies against Y876 (pY876) and S880 (pS880). Representative immunoblot images are shown in *Upper*. In *Lower*, intensities of pY876 and pS880 bands in K-glu–treated slices were normalized to those band intensities in untreated slices. The bar represents mean and SEM. $*P < 0.05$; $**P < 0.01$, respectively ($n = 8$ each for WT and $n = 13$ each for *GluD2*-null cerebellum). (*C* and *D*) Y876 phosphorylation inhibits subsequent S880 phosphorylation in the in vitro phosphorylation assay. The C-terminal region of GluA2 was conjugated with GST (GST-GluA2-CT). Y876 was replaced with phenylalanine to produce GST-GluA2^{YF}-CT. (*C*) GST-GluA2-CT or (*D*) GST-GluA2^{Y876F}-CT was incubated with Src or boiled Src followed by PKC. Phosphorylation of GluA2 was detected by antiphospho-Y876– and antiphospho-S880–specific antibodies. Representative immunoblot images are shown in *Upper*. The diagrams show intensities of S880 phosphorylation levels (pS880) with prior Src treatment (+Src) normalized by intensities of pS880 with boiled Src (Ctl). Intensities of Y876 phosphorylation levels (pY876) with subsequent PKC treatment (+PKC) normalized by intensities of pY876 without Src (Ctl) are also shown. The bar represents mean and SEM. $**P < 0.01$ ($n = 11$ for pY876 and $n = 13$ for pS880). (*E*) Inhibition of tyrosine phosphorylation restores K-glu–evoked changes in Y876 and S880 phosphorylation in *GluD2*-null cerebellum. Cerebellar slices from *GluD2*-null mice were preincubated with a PP1 analog for 15 min and then treated with K-glu in the presence of a PP1 analog. K-glu treatment significantly decreased Y876 phosphorylation and increased S880 phosphorylation in *GluD2*-null cerebellum. Representative immunoblot images are shown in *Upper*. In *Lower*, intensities of pY876 and pS880 bands in K-glu–treated slices were normalized to those band intensities in untreated slices. The bar represents mean and SEM. $*P < 0.05$ ($n = 16$ for pY876 and $n = 17$ for pS880).

8 each, $P < 0.01$) (Fig. 2*A*). K-glu treatment failed to induce changes in the phosphorylation levels of Y876 in *GluD2*-null cerebellar slices (0.93 ± 0.11-fold vs. control, $n = 13$ each, $P = 0.50$) (Fig. 2*B*). Thus, the basal phosphorylation levels of tyrosine had not only increased but also remained high after stimulation with K-glu in *GluD2*-null cerebellum.

Increased Y876 Phosphorylation Inhibited Activity-Induced S880 Phosphorylation in *GluD2*-Null Purkinje Cells. K-glu treatment failed to phosphorylate S880 and dephosphorylate Y876 in *GluD2*-null cerebellum. These two sites are located close to each other (Fig. 1*A*); therefore, we hypothesized that Y876 phosphorylation may interfere with subsequent S880 phosphorylation. To examine this hypothesis, we first performed an in vitro phosphorylation assay of the GluA2 C-terminal region that was fused to GST (GST-GluA2-CT). Immunoblot analyses with phosphorylation-specific antibodies confirmed that the GST-GluA2-CT was phosphorylated at Y876 and S880 in vitro by purified Src and PKC, respectively. Prior treatment of GST-GluA2-CT with Src, but not boiled Src, significantly decreased the subsequent S880 phosphorylation levels by PKC (0.66 ± 0.06-fold vs. boiled Src treatment, $n = 13$, $P < 0.001$), whereas the addition of PKC itself did not affect the phosphorylation levels of Y876 (Fig. 2*C*). In contrast, when Y876 was replaced with nonphosphorylatable phenylalanine (GST-GluA2^{Y876F}-CT), prior treatment with Src did not affect subsequent S880 phosphorylation by PKC (1.15 ± 0.13-fold vs. boiled Src treatment, $n = 6$, $P = 0.13$) (Fig. 2*D*). These results indicated that the phosphorylation of Y876 in GluA2 specifically regulated the subsequent phosphorylation of S880 by PKC in vitro.

To further examine this hypothesis in a cellular context, we pretreated *GluD2*-null cerebellar slices with a PP1 analog to reduce the increased basal tyrosine phosphorylation levels and examined whether K-glu treatment could induce S880 phosphorylation under such conditions. Immunoblot analyses confirmed that preincubation with the PP1 analog significantly reduced the basal phosphorylation levels of Y876 without affecting S880 phosphorylation in *GluD2*-null cerebellar slices (Fig. S2), indicating that basal Y876 phosphorylation levels were determined by the balance between endogenous SFK and phosphatase activities. As observed in WT cerebellar slices (Fig. 2*A*), subsequent K-glu treatment induced an increase in S880 phosphorylation levels (1.37 ± 0.19-fold vs. control, $n = 17$, $P = 0.04$) in *GluD2*-null cerebellar slices that had been pretreated with a PP1 analog (Fig. 2*E*). These results indicated that the increased basal phosphorylation of Y876 in GluA2 was responsible for the reduced S880 phosphorylation by K-glu in *GluD2*-null cerebellum.

Rescue of Impaired LTD in *GluD2*-Null Purkinje Cells by the Inhibition of the Phosphorylation of Y876 in GluA2. To establish the causal relationship between the increased Y876 phosphorylation levels and impaired LTD, we applied a PP1 analog to *GluD2*-null Purkinje cells using a patch pipette. The inclusion of a PP1 analog did not affect the baseline PF-evoked AMPA receptor-mediated EPSCs (PF-EPSCs) (Fig. S3) in WT and *GluD2*-null Purkinje cells. In addition, the application of conjunctive stimulation (CJ-stim; 30 cycles of PF stimulation plus Purkinje cell depolarization at 1 Hz) robustly induced LTD in WT Purkinje cells with (Fig. 3 *B* and *C*) (72 ± 5% at 25–30 min after CJ-stim, $n = 8$) or without a PP1 analog (Fig. 3 *A* and *C*) (74 ± 4% at 25–30 min after CJ-stim, $n = 9$, $P = 0.56$ vs. with a PP1 analog). In contrast, although CJ-stim failed to induce LTD in *GluD2*-null Purkinje cells (Fig. 3 *D* and *F*) (99 ± 2% at 25–30 min after CJ-stim, $n = 8$) as reported previously (2), it induced LTD in Purkinje cells with a PP1 analog (Fig. 3 *E* and *F*) (80 ± 5% at 25–30 min after CJ-stim, $n = 10$; $P = 0.006$ vs. without PP1 analog). These results indicated that impaired LTD in *GluD2*-null Purkinje cells was successfully rescued by the application of a PP1 analog to Purkinje cells and that increased tyrosine phosphorylation was responsible for the impaired LTD in *GluD2*-null Purkinje cells.

A PP1 analog could affect the tyrosine phosphorylation of many proteins in Purkinje cells. Thus, to examine the specific role of GluA2 phosphorylation at Y876 in LTD, we expressed GluA2 mutants, in which the tyrosine phosphorylation sites were disrupted, with a Sindbis virus vector in *GluD2*-null Purkinje cells. CJ-stim failed to induce LTD in *GluD2*-null Purkinje cells expressing WT GluA2 (Fig. 3 *G* and *J*) (89 ± 6% at 25–30 min after CJ-stim, $n = 6$) or mutant GluA2, in which phenylalanine replaced the two tyrosine residues at 869 and 873 (Fig. 3 *I* and *J*) (GluA2^{Y869F,Y873F}; 91 ± 6% at 25–30 min after CJ-stim, $n = 6$). In contrast, CJ-stim induced LTD in *GluD2*-null Purkinje cells expressing mutant GluA2, in which phenylalanine replaced the tyrosine at 876 (Fig. 3 *H* and *J*) (GluA2^{Y876F}; 66 ± 5% at 25–30 min after CJ-stim, $n = 5$, $P = 0.038$ vs. GluA2^{WT} and $P = 0.048$ vs. GluA2^{Y869F,Y873F}). Surface biotinylation assays showed that the cell surface expression levels of GluA2^{Y876F} and GluA2^{Y869F,Y873F} were comparable with the cell surface expression levels of WT GluA2 in human embryonic kidney 293 (HEK293) cells (Fig. S4). These results indicated that increased phosphorylation at Y876, but not at other tyrosine residues, at the C terminus of GluA2 was responsible for the impaired LTD, and its dephosphorylation was sufficient to restore LTD in *GluD2*-null mice.

Phosphorylation of Y876 Inhibited LTD Independent of the BRAG2-Arf6 Pathway in the Cerebellum. Recently, brefeldin-resistant Arf-guanine nucleotide exchange factor 2 (BRAG2), which activates Arf6, has been shown to bind to the C terminus of GluA2 in a manner that is dependent on Y876 dephosphorylation, and it, thereby, regulates AMPA receptor endocytosis at hippocampal synapses during LTD (14). Thus, the increased Y876 phosphorylation in *GluD2*-null Purkinje cells may inhibit the BRAG2-Arf6 pathway in addition to S880 phosphorylation. To examine this possibility, we used synthetic peptides that were derived from the C terminus sequence of GluA2 between positions 869 and 877 (^{869}**Y**KEG**Y**NV**Y**G^{877}) (Fig. 4*A*), which contained three tyrosine residues. The unphosphorylated peptides (pep-3Y), but not the unphosphorable peptides (pep-3A), in which alanine replaced the three tyrosine residues, have previously been shown to inhibit LTD induction in the amygdala (23), nucleus accumbens (24), and hippocampus (11, 14). In those studies, pep-3Y may have inhibited LTD induction by serving as a decoy peptide for BRAG2 (14) or a pseudosubstrate for SFKs (16). In contrast to the previous reports, the application of these peptides to WT Purkinje cells through a patch pipette did not affect CJ-stim–induced LTD in the cerebellum (Fig. 4 *B*, *D*, and *E*) (66 ± 4% and 69 ± 7% at 25–30 min after CJ-stim in pep-3Y and pep-3A, respectively, $n = 8$ each). Instead, the application of phosphorylated peptides, in which all of the tyrosine residues were phosphorylated (pep-3pY), significantly inhibited LTD induction in WT Purkinje cells (Fig. 4 *C* and *E*) (90 ± 6% at 25–30 min after CJ-stim, $n = 8$, $P = 0.035$ vs. pep-3Y and $P = 0.047$ vs. pep-3A). We did not detect any differences in the EPSC amplitudes just after breaking into whole-cell mode and 9–10 min later in any of the experiments with the peptides (Fig. S5), suggesting that the peptides did not affect basal PF–Purkinje cell synaptic transmission. Because BRAG2 does not bind to phosphorylated GluA2 peptides (14), these results suggested that the BRAG2-Arf6 signaling pathway may not play a major role in CJ-stim–induced LTD in Purkinje cells. Instead, pep-3pY most probably served as a pseudosubstrate for tyrosine phosphatases. Thus, the increased Y876 phosphorylation in *GluD2*-null Purkinje cells inhibited LTD induction mainly by preventing S880 phosphorylation.

***PTPMEG*-Null and *GluD2*-Null Cerebellum Exhibited Similar GluA2 Phosphorylation Patterns.** *GluD2*-null mice show increased phosphorylation of Y876 in GluA2. The C-terminal domain of GluD2

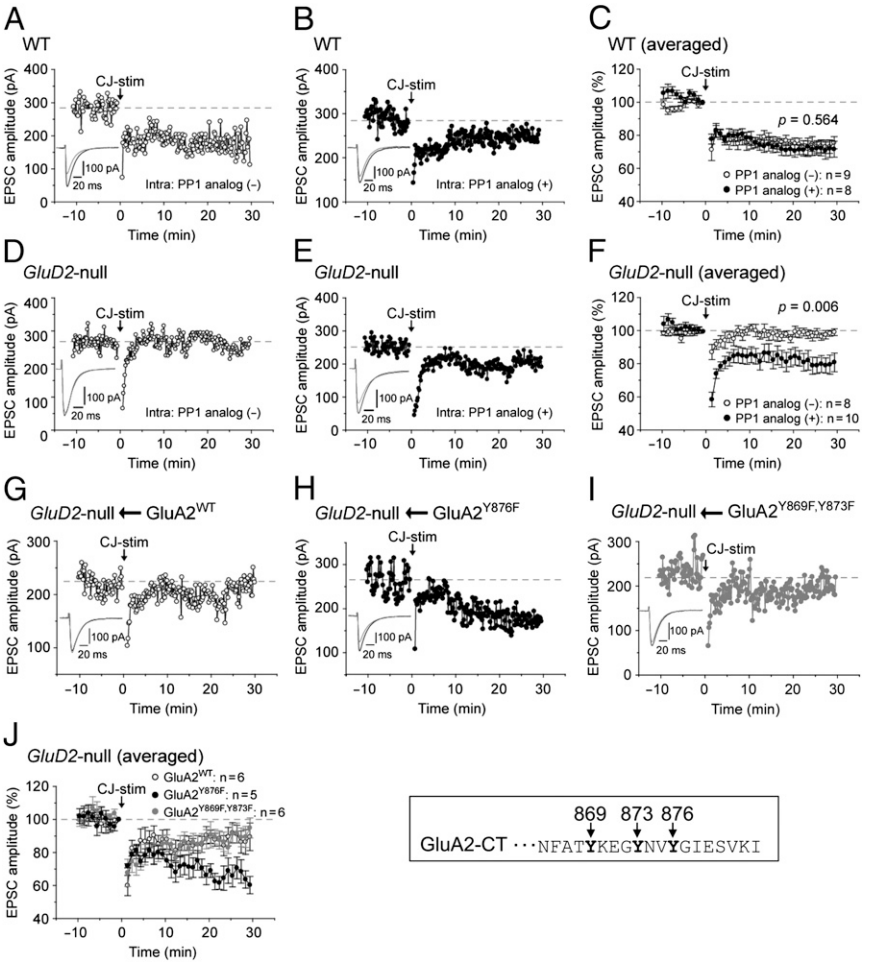

Fig. 3. Dephosphorylation of tyrosine of GluA2 is sufficient to restore LTD induction in *GluD2*-null Purkinje cells. (*A–F*) Inclusion of a PP1 analog in a patch pipette restored LTD in *GluD2*-null Purkinje cells, but it did not affect LTD in WT Purkinje cells. Application of CJ-stim (consisting of 30 cycles of PF stimulation plus Purkinje cell depolarization at 1 Hz) induced LTD in WT Purkinje cells with (+) or without (–) a PP1 analog (10 μM) in patch pipettes (*A* and *B*). CJ-stim successfully induced LTD in *GluD2*-null Purkinje cells with (*E*; +) but not without (*D*; –) a PP1 analog. Collective results (mean and SEM) are shown in *C* and *F*. *Insets* sweeps in *A*, *B*, *D*, and *E* show PF-EPSCs just before (black traces) and 30 min after (gray traces) CJ-stim. (*G–J*) Overexpression of unphosphorable GluA2 subunits restored LTD induction in *GluD2*-null Purkinje cells. Y869, Y873, and Y876 phosphorylation sites (shown on the right in *J*) were replaced with phenylalanine to produce unphosphorable GluA2 mutants termed as $GluA2^{Y876F}$ and $GluA2^{Y869F,Y873F}$. $GluA2^{WT}$, $GluA2^{Y876F}$, and $GluA2^{Y869F,Y873F}$ were overexpressed in *GluD2*-null Purkinje cells by a Sindbis virus vector. CJ-stim–induced LTD was restored in *GluD2*-null Purkinje cells expressing $GluA2^{Y876F}$ (*H*) but not Purkinje cells expressing $GluA2^{WT}$ (*G*) or $GluA2^{Y869F,Y873F}$ (*I*). Collective data (mean and SEM) are shown in *J*. *Insets* sweeps in *G–I* show PF-EPSCs just before (black traces) and 30 min after (gray traces) CJ-stim.

plays a crucial role in LTD induction (3, 4); therefore, we first examined whether the C terminus of GluD2 regulated tyrosine phosphorylation at PF–Purkinje cell synapses by measuring $_{slow}$EPSCs. We used transgenic mice that expressed WT GluD2 (*Tg*WT) or mutant GluD2, which lacked the seven C-terminal residues (*Tg*ΔCT7) on a *GluD2*-null background. In contrast to *GluD2*-null mice, the numbers of PF–Purkinje cell synapses and climbing fiber innervation patterns have previously been shown to be comparable between *GluD2*-null/*Tg*ΔCT7 and *GluD2*-null/*Tg*WT cerebellum (4). Nevertheless, the amplitudes and transferred charges of $_{slow}$EPSCs were significantly smaller in *GluD2*-null/*Tg*ΔCT7 Purkinje cells than *GluD2*-null/*Tg*WT Purkinje cells (Fig. 5*A*) ($P = 0.001$ for amplitudes and $P = 0.001$ for transferred charges). These results indicated that the C terminus of GluD2, to which various intracellular PDZ proteins bind, played a crucial role in the regulation of tyrosine phosphorylation levels in Purkinje cells.

Among the various PDZ proteins that bind to the C terminus of GluD2, we focused on PTPMEG, because it has a catalytically active protein tyrosine phosphatase domain (15) that could potentially serve as a link between the C terminus of GluD2 and the tyrosine phosphorylation levels of Purkinje cells. In addition, *PTPMEG*-null mice displayed impaired motor learning and abrogated LTD (25), although the underlying mechanisms remain unknown. Thus, we first examined the basal phosphorylation levels of GluA2 in *PTPMEG*-null mice. Immunoblot analyses of the synaptosomal fraction revealed that Y876 phosphorylation was significantly increased in *PTPMEG*-null cerebellum compared with WT cerebellum (Fig. 5*B*) (1.84 ± 0.35-fold vs. WT, $n = 10$ each, $P = 0.04$), whereas no differences were observed in the phosphorylation levels of S880 between WT and *PTPMEG*-null cerebellum (Fig. 5*C*) (1.05 ± 0.42-fold vs. WT, $n = 7$ each, $P = 0.85$). Furthermore, K-glu treatment failed to induce a decrease in Y876 phosphorylation (0.99 ± 0.15-fold vs. WT, $n = 15$, $P = 0.97$) and an increase in S880 phosphorylation (0.86 ± 0.14-fold vs. WT, $n = 15$, $P = 0.36$) in *PTPMEG*-null cerebellar slices (Fig. 5*D*). These results were very similar to results that were observed in *GluD2*-null cerebellar slices (Figs. 1*B* and 2*B*), and they suggested that it was PTPMEG that bound to the C ter-

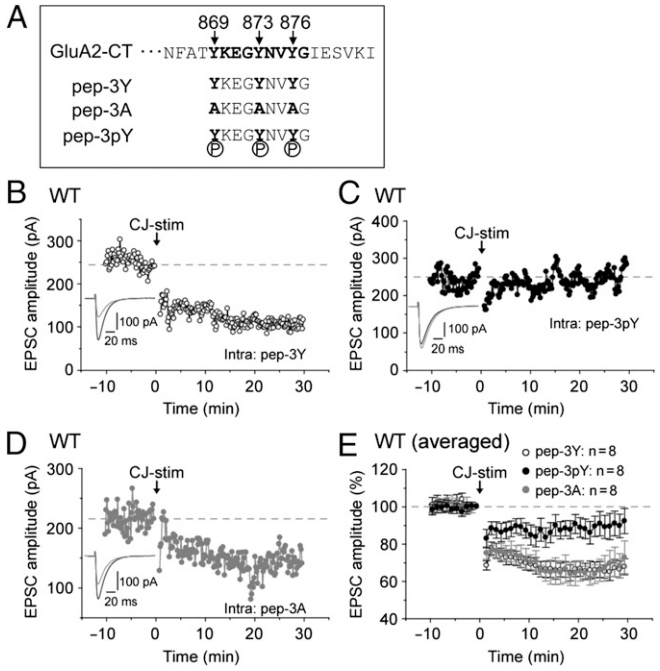

Fig. 4. Dephosphorylation of tyrosine of GluA2 is necessary for LTD induction in WT Purkinje cells. (*A*) Diagram indicating three peptides used in this study. Synthetic peptides correspond to the GluA2 C terminus between positions 869 and 877. Alanine replaced three tyrosine residues in the original peptide (pep-3Y) to produce unphosphorable peptide (pep-3A). All tyrosine residues were phosphorylated in pep-3pY. (*B–E*) LTD is specifically inhibited by pep-3pY, which could serve as a pseudosubstrate for tyrosine phosphatase, included in Purkinje cells. Inclusion of pep-3Y (*B*) or pep-3A (*D*) in patch pipettes did not affect CJ-stim–induced LTD in WT Purkinje cells, but pep-3pY (*C*) inhibited LTD induction. Collective data (mean and SEM) are shown in *E*. *Inset* sweeps show PF-EPSCs before and 30 min after CJ-stim.

minus of GluD2 and regulated the tyrosine phosphorylation at PF–Purkinje cell synapses.

Interactions with PTPMEG Were Necessary and Sufficient for GluD2 to Induce LTD. To further clarify the significance of the interactions between GluD2 and PTPMEG in regulating LTD, we expressed mutant GluD2 that lacked the seven C-terminal residues (GluD2ΔCT7), which did not bind PTPMEG (15) in *GluD2*-null Purkinje cells. As previously reported, unlike WT GluD2 (3), GluD2ΔCT7 did not rescue the impaired LTD in *GluD2*-null Purkinje cells (Fig. 6 *A* and *C*) (90 ± 8% at 25–30 min after CJ-stim, $n = 8$). In contrast, when GluD2ΔCT7-PTP, in which the catalytic phosphatase domain of PTPMEG was fused to the C terminus of GluD2ΔCT7, was expressed in *GluD2*-null Purkinje cells, CJ-stim successfully induced LTD (Fig. 6 *B* and *C*) (76 ± 6% at 25–30 min after CJ-stim, $n = 11$, $P = 0.04$ vs. GluD2ΔCT7). These results suggested that the presence of the phosphatase domain of PTPMEG near GluD2 was sufficient to restore the impaired LTD in *GluD2*-null Purkinje cells.

To examine whether interactions between endogenous GluD2 and PTPMEG were necessary for LTD induction in WT Purkinje cells, we expressed an inactive phosphatase mutant of PTPMEG (PTPMEG^{DA}; see next section) with a Sindbis virus vector in WT Purkinje cells. Because CJ-stim no longer induced LTD in WT cells expressing PTPMEG^{DA} (Fig. 6 *D* and *F*) (89 ± 4% at 25–30 min after CJ-stim, $n = 8$), PTPMEG^{DA} probably exerted a dominant-negative effect on endogenous PTPMEG. In contrast, the expression of another mutant (PTPMEG^{DA}-ΔPDZ), which lacked the PDZ domain that was necessary for binding to GluD2 (15), no longer inhibited LTD induction in WT Purkinje cells (Fig. 6 *E* and *F*) (66 ± 4% at 25–30 min after CJ-stim, $n = 9$, $P = 0.004$ vs. PTPMEG^{DA}). These results indicated that direct interactions between GluD2 and PTPMEG and its phosphatase activity at postsynaptic sites were necessary and sufficient for LTD induction in Purkinje cells.

GluA2, a Substrate for PTPMEG. Finally, to examine whether GluA2 served as a substrate for PTPMEG, we performed a substrate-trapping assay. Various substrates of tyrosine phosphatases have been identified with substrate-trapping mutants, in which mutations in the catalytic center abrogate their enzymatic activity by trapping substrates (26). For example, a substrate-trapping mutant of protein tyrosine phosphatase H1 (PTPH1), which is the most closely related phosphatase to PTPMEG in the phylogenetic tree, has been produced by replacing aspartate with alanine in the catalytic center, and it has been used to identify valosin-containing protein (VCP) as a substrate (27). Thus, we introduced similar mutations in the catalytic center of PTPMEG to produce the possible trapping mutant PTPMEG^{DA}, in which alanine (A) replaced aspartate (D). Because many proteins are phosphory-

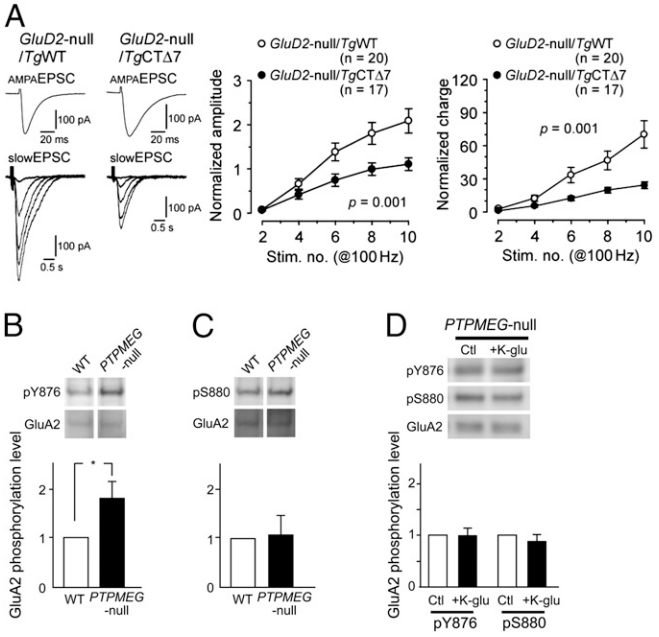

Fig. 5. PTPMEG regulates tyrosine dephosphorylation levels at PF–Purkinje cell synapses. (*A*) Seven C-terminal amino acids of GluD2 determine $_{slow}$EPSC amplitudes in Purkinje cells. $_{slow}$EPSCs were evoked in *GluD2*-null Purkinje cells expressing WT GluD2 transgenes (*GluD2*-null/*Tg*WT) or mutant GluD2 transgenes lacking the seven C-terminal amino acids (*GluD2*-null/*Tg*CTΔ7) as described in Fig. 1C. Representative traces are shown in *Left*. Amplitudes and charges of $_{slow}$EPSCs were normalized by amplitudes and charges of $_{AMPA}$EPSCs and plotted against the number of stimulations in *Right*. The bar represents mean and SEM. (*B* and *C*) Basal phosphorylation of Y876 and S880 of GluA2 subunits in *PTPMEG*-null mice. Representative immunoblot images of the synaptosomal fraction of WT and *PTPMEG*-null cerebellum using an antibody against pY876 or pS880 are shown in *Upper*. *Lower* shows intensities of pY876 bands (*B*) or pS880 bands (*C*) in *PTPMEG*-null cerebellum normalized by those band intensities in WT cerebellum. Basal phosphorylation of Y876, but not S880, was significantly increased in *PTPMEG*-null cerebellum. The bar represents mean and SEM. *$P < 0.05$ ($n = 10$ for Y876; $n = 7$ for S880). (*D*) Chemical LTD stimulus induces no changes at Y876 and S880 sites in *PTPMEG*-null cerebellum. *PTPMEG*-null cerebellar slices were treated with 50 mM KCl plus 10 μM L-glutamate for 5 min (K-glu), and the cell lysates were subjected to immunoblot analyses using phosphorylation-specific antibodies against pY876 and pS880. Representative immunoblot images are shown in *Upper*. In *Lower*, intensities of pY876 and pS880 bands in K-glu–treated slices were normalized to those band intensities in untreated slices. The bar represents mean and SEM ($n = 15$ each).

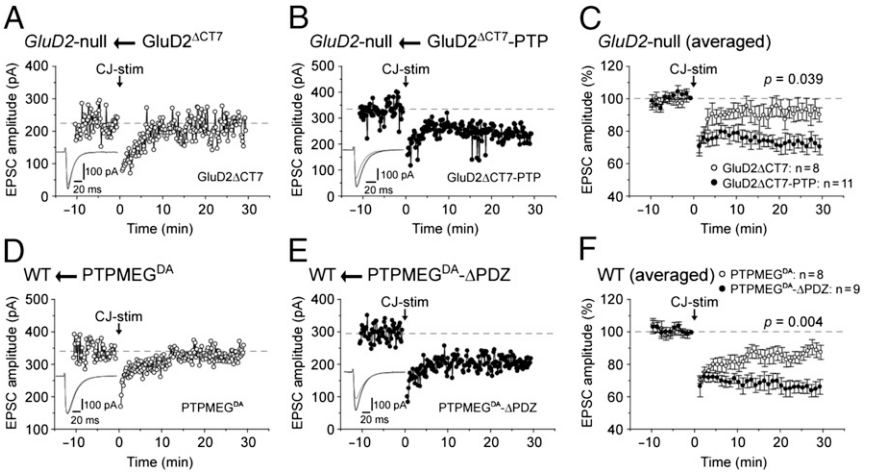

Fig. 6. Interaction of GluD2 with enzymatically active PTPMEG is necessary for LTD induction. (*A–C*) The catalytic domain of PTPMEG was sufficient to restore LTD in *GluD2*-null mice. The catalytic phosphatase domain of PTPMEG was directly fused to the C terminus of a mutant GluD2 lacking the seven C-terminal amino acids (GluD2$^{\Delta CT7}$) to produce GluD2$^{\Delta CT7}$-PTP. GluD2$^{\Delta CT7}$ and GluD2$^{\Delta CT7}$-PTP were expressed in *GluD2*-null Purkinje cells by the Sindbis virus vector. CJ-stim induced LTD in *GluD2*-null Purkinje cells expressing GluD2$^{\Delta CT7}$-PTP (*B*) but not Purkinje cells expressing GluD2$^{\Delta CT7}$ (*A*). Collective data (mean and SEM) are shown in *C*. *Insets* sweeps show PF-EPSCs just before (black traces) and 30 min after (gray traces) CJ-stim. (*D–F*) Interaction with endogenous PTPMEG is necessary for LTD in WT Purkinje cells. A phosphatase-inactive mutant PTPMEG (PTPMEG^{DA}) was produced by replacing aspartate in the catalytic domain with alanine. The PDZ domain, by which PTPMEG binds to the C terminus of GluD2, was further deleted to produce PTPMEG^{DA}-ΔPDZ. PTPMEG^{DA} or PTPMEG^{DA}-ΔPDZ was transduced into WT Purkinje cells using a Sindbis virus vector. CJ-stim–evoked LTD was inhibited in Purkinje cells expressing PTPMEG^{DA} (*D*) but not Purkinje cells expressing PTPMEG^{DA}-ΔPDZ (*E*), indicating that PTPMEG^{DA} bound to GluD2 and replaced endogenous PTPMEG as a dominant-negative molecule. Collective data (mean and SEM) are shown in *F*. *Insets* sweeps show PF-EPSCs just before (black traces) and 30 min after (gray traces) CJ-stim.

lated at tyrosine residues by endogenous tyrosine kinase activities in HEK293 cells, the lysate of HEK293 cells was pulled down by the GST that was fused with the catalytic domain of WT PTPMEG (GST-PTP^{WT}) or PTPMEG^{DA} (GST-PTP^{DA}). As reported for PTPH1 (27), GST-PTP^{DA} but not GST-PTP^{WT} pulled down endogenous VCP in HEK293 cells (Fig. 7*A*). In contrast, unlike VCP, endogenous *N*-ethylmaleimide–sensitive factor, which is a member of the ATPase family that is associated with a variety of cellular activities, did not interact with GST-PTP^{DA} (Fig. 7*A*), indicating that PTP^{DA} specifically trapped its substrates. GST-PTP^{DA} also pulled down GluA2 from the lysate of HEK293 expressing GluA2 (Fig. 7*A*), suggesting that GluA2 was a substrate for PTPMEG.

To examine whether PTPMEG directly dephosphorylated tyrosine residues at the C terminus of GluA2, we performed an in vitro dephosphorylation assay with pep-3pY as a substrate (Fig. 4*A*). GST-PTP^{DA} and GST-PTP^{CS}, having cysteine (C) residue in the catalytic center that was replaced with serine (S), were used as PTPMEG mutants with reduced phosphatase activities. Isobaric tag-based mass spectrometric quantification of the phosphorylation of pep-3pY peptides revealed that all tyrosine residues were dephosphorylated by incubation with GST-PTP^{WT} (0.06 ± 0.02-fold compared with pep-3pY peptides incubated with GST only, $n = 6$) (Fig. 7*B*). In contrast, the relative phosphorylation levels of pep-3pY, which was incubated with GST-PTP^{DA} (1.1 ± 0.3, $n = 6$) or GST-PTP^{CS} (1.0 ± 0.1, $n = 6$), were significantly higher than those levels treated with PTP^{WT} (WT vs. DA or CS, $P < 0.05$) (Fig. 7*B*). These results indicated that the phosphorylated tyrosine residues in the GluA2 C terminus were directly dephosphorylated by PTPMEG in vitro.

To further confirm that PTPMEG dephosphorylated Y876 in GluA2 in a cellular context, we examined whether full-length PTPMEG dephosphorylated GluA2 in HEK293 cells. Immunoblot analyses of the lysate of HEK293 cells transfected with GluA2 revealed that GluA2 was weakly phosphorylated at Y876 by endogenous tyrosine kinases in HEK293 cells. We found that Y876 phosphorylation levels were significantly higher in HEK293 cells that coexpressed a phosphatase-inactive mutant PTPMEG^{DA} (3.6 ± 0.9-fold vs. PTPMEG^{WT}, $n = 8$ each, $P < 0.05$) (Fig. 7*C*) than cells that coexpressed PTPMEG^{WT} or an empty vector (1.4 ± 0.3-fold vs. PTPMEG^{WT}, $n = 8$ each, $P < 0.05$) (Fig. 7*C*). There was no statistically significant difference in the phosphorylation levels of Y876 between the cells expressing PTPMEG^{WT} and an empty vector, suggesting that endogenous tyrosine phosphatase dephosphorylated Y876 in HEK293 cells. These results indicated that Y876 in GluA2 served as a direct substrate for PTPMEG.

Discussion

LTD at PF–Purkinje cell synapses is believed to play important roles in motor learning in the cerebellum, and it has been shown to absolutely require functional GluD2 in Purkinje cells (28). Nevertheless, how and why GluD2 regulates LTD in the cerebellum remain elusive. In this study, we show that the basal phosphorylation levels of Y876 in GluA2 were increased (Fig. 1) and that the phosphorylation at Y876 prevented subsequent phosphorylation at S880 (Fig. 2), which has been shown to be an essential phosphorylation site for AMPA receptor endocytosis during LTD in both hippocampus (6, 7) and cerebellum (8–10). Dephosphorylation of Y876 restored AMPA receptor endocytosis (Fig. 2) and LTD (Fig. 3) in *GluD2*-null mice. An association of PTPMEG with the C terminus of GluD2 was necessary and sufficient for LTD induction in Purkinje cells (Figs. 3, 4, 5, and 6). Furthermore, PTPMEG directly dephosphorylated Y876 phosphorylation of GluA2 (Fig. 7). Therefore, we propose that GluD2 serves as a master switch in gating the inducibility of LTD by coordinating the interactions between the two phosphorylation sites in GluA2 through its interactions with PTPMEG (Fig. 8).

Interactions Between Y867 and S880 Phosphorylation During LTD. Whether tyrosine phosphorylation is involved in cerebellar LTD has been controversial. In early studies, cerebellar LTD has been reported to be blocked by broad-spectrum tyrosine kinase inhibitors, such as genistein and lavendustin A, suggesting that LTD depends on tyrosine phosphorylation events (29, 30). In contrast, the application of a more specific Src inhibitor PP2 to the bath solution (31) or PP1 to a patch pipette (Fig. 3 *A–C*) did not affect

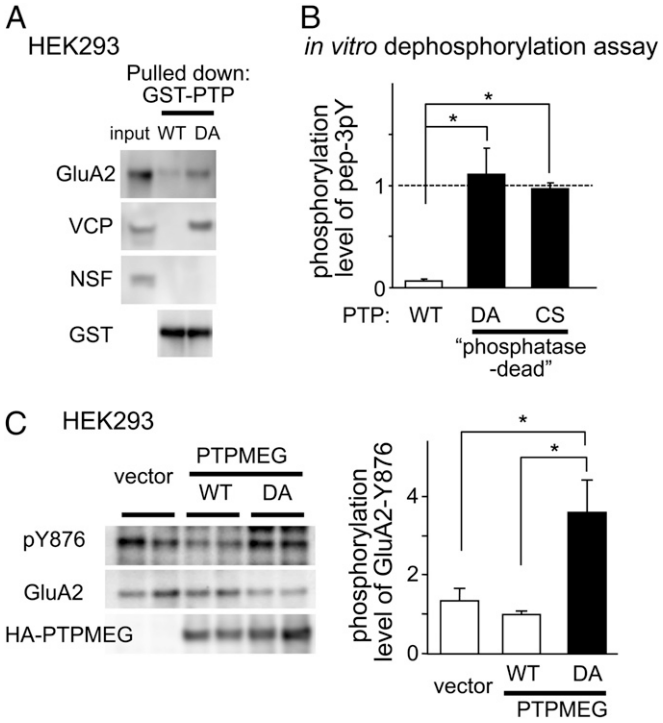

Fig. 7. GluA2 is a substrate of PTPMEG. (*A*) A substrate-trap mutant of PTPMEG interacts with GluA2. The cell lysate of HEK293 cells transfected with GluA2 was pulled down with the catalytic domain of PTPMEG fused with GST (GST-PTP). Aspartate in the catalytic center was replaced with alanine to produce a substrate-trap mutant (GST-PTP^{DA}). As reported for a related phosphatase PTPH1, endogenous VCP was trapped by GST-PTP^{DA} but not GST-PTP. *N*-ethylmaleimide–sensitive factor (NSF), a protein related to VCP, was not pulled down by GST-PTP^{DA} or GST-PTP. Similarly, GluA2 was more effectively pulled down by GST-PTP^{DA}. (*B*) GluA2 C-terminal peptides are directly dephosphorylated by PTPMEG in vitro. Cysteine in the catalytic center was replaced with serine to produce another substrate trap mutant (GST-PTP^{CS}). A tyrosine-phosphorylated synthetic peptide, pep-3pY, derived from the C terminus (869–877) of GluA2 was incubated with GST-PTP, GST-PTP^{DA}, GST-PTP^{CS}, or GST alone and subjected to the isobaric tag-based quantitative mass spectrometric analyses. The diagram indicates phosphorylation levels of peptides treated with each GST-fusion protein normalized by phosphorylation levels of peptides treated with GST alone. Bars represent mean and SEM. $^*P < 0.05$ ($n = 6$ for each group). (*C*) PTPMEG dephosphorylates Y876 of GluA2 in HEK293 cells. GluA2 and WT or a phosphatase-inactive mutant (DA) PTPMEG were coexpressed in HEK293 cells, and the cell lysates were subjected to immunoblot analyses using a phosphorylation-specific antibody against pY876. Representative immunoblot images are shown in *Left*. *Right* shows intensities of pY876 bands normalized by those band intensities in cells expressing WT PTPMEG. Phosphorylation levels of Y876 of GluA2 were significantly higher in cells coexpressing a phosphatase-inactive mutant PTPMEG. The bar represents mean and SEM. $^*P < 0.05$ ($n = 8$ for each group).

LTD induction in WT Purkinje cells. Conversely, the inclusion of purified Src in the patch pipette blocked LTD induction in Purkinje cells (31). Furthermore, the phosphorylation levels of Y876 in GluA2 were reduced in the synaptosomal fraction of WT cerebellar slices after chemical LTD by K-glu treatment (Fig. 2*A*). These results indicated that, similar to mGluR-dependent LTD in the hippocampus (32, 33), cerebellar LTD, which is also dependent on the mGluR, was accompanied by dephosphorylation of Y876 in GluA2.

By studying *GluD2*-null and *PTPMEG*-null cerebellum, we found unexpected interactions between the Y876 and S880 phosphorylation sites in GluA2. When basal phosphorylation levels of Y876 increased in *GluD2*-null (Fig. 1*B*) or *PTPMEG*-null (Fig. 5*B*) cerebellum, K-glu treatment failed to increase S880 phosphorylation (Figs. 2*B* and 5*D*). The application of a PP1 analog not only reduced the basal phosphorylation levels of Y876 but also restored K-glu–induced S880 phosphorylation (Fig. 2*E*) and CJ-stim–induced LTD (Fig. 3 *D*–*F*) in *GluD2*-null Purkinje cells. In addition, LTD was restored in *GluD2*-null Purkinje cells that expressed GluA2^{Y876F} (Fig. 3 *G*–*J*). Similar interactions between serine and tyrosine phosphorylation sites have been reported in other signaling molecules. For example, the serine phosphorylation of the insulin receptor substrate has been shown to hinder its tyrosine phosphorylation levels (34). The serine phosphorylation of the C terminus of the NMDA receptor subunit GluN2B also interferes with subsequent phosphorylation at a closely located tyrosine residue (35). However, in these cases, dissociation of the interacting proteins by serine phosphorylation affects local tyrosine phosphorylation. In contrast, the phosphomimetic peptide pep-3pY, which should facilitate LTD induction by competing for such interacting proteins, inhibited LTD induction in WT Purkinje cells (Fig. 4 *C* and *E*). Furthermore, an in vitro phosphorylation assay revealed that Y876 phosphorylation by Src specifically inhibited S880 phosphorylation by PKC in vitro (Fig. 2 *C* and *D*). These results indicated that S880 phosphorylation was inhibited by Y876 phosphorylation on single AMPA receptors through direct mechanisms, such as conformation changes or electrostatic charges that are associated with Y876 phosphorylation. Additional structural studies are warranted to clarify these unique interactions between the Y876 and S880 phosphorylation sites in GluA2.

The dephosphorylation of Y876 in GluA2 plays an essential role in hippocampal LTD that is induced by the mGluR agonist 3,4-dihydroxyphenylglycine (32, 33). The specific binding of BRAG2 to dephosphorylated Y876 has been shown to regulate AMPA receptor endocytosis in hippocampal neurons by activating Arf6, which turns on phosphatidylinositol 4-phosphate 5-kinase (PIP5K) to produce phosphatidylinositol (4,5)-bisphosphate and recruit adaptor protein-2 and clathrin (14). In contrast to hippocampal LTD, however, cerebellar LTD was not inhibited by the application of pep-3A (Fig. 4 *D* and *E*), which competes for BRAG2 (14). Thus, the BRAG2-Arf6 pathway may not play a major role in cerebellar LTD. Because the accumulation of adaptor protein-2 and clathrin has been shown to be required for AMPA receptor endocytosis during cerebellar LTD (9), we suspect that PIP5K may be activated by other pathways. For example, PIP5K could be activated by calcineurin in low-frequency stimulation-induced LTD in the hippocampus (36). Interestingly, PTPMEG has been shown to also be expressed in the hippocampus (15). In addition, GluD1, which is a GluD2 family member that also binds PTPMEG (Fig. S6), has been shown to be expressed in the hippocampus (37). Considering that the phosphorylation of S880 in GluA2 has been shown to be involved in hippocampal LTD under certain conditions (7, 38), we suggest that Y876 dephosphorylation could also regulate hippocampal LTD induction by direct interactions with the S880 sites in GluA2, which was observed in Purkinje cells.

Regulation of LTD by GluD2-PTPMEG Signaling. In addition to PTPMEG, other proteins, such as delphilin, bind to the C terminus of GluD2. Notably, both motor learning and LTD induction are facilitated in mice lacking delphilin (39). The FH1 domain of delphilin binds to the SH3 domain of Src in a yeast two-hybrid system (40). In addition, we found that SFK was coimmunoprecipitated with delphilin in transfected HEK293 cells (Fig. S7). Thus, although the regulation of the binding of PTPMEG and delphilin is unclear, we suggest that delphilin binding may up-regulate the phosphorylation of Y876 in GluA2 and inhibit LTD, whereas PTPMEG binding down-regulates Y876 phosphorylation and enhances LTD. Thus, Y876 phosphorylation levels, regulated by the C terminus of GluD2, may serve as a regulator of metaplasticity at PF–Purkinje cell synapses in determining LTD inducibility.

Although striatal-enriched protein tyrosine phosphatase (STEP) has been shown to play a crucial role in 3,4-dihydroxyphenylglycine–induced mGluR-dependent LTD in the hippocampus (41), it

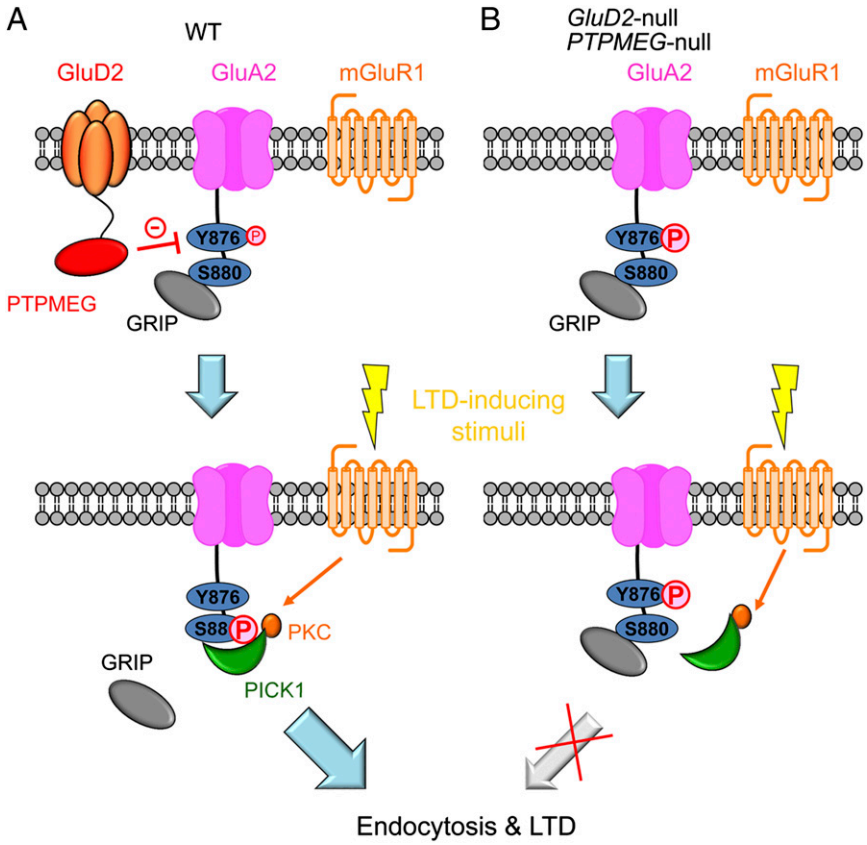

Fig. 8. A proposed role of GluD2 in the regulation of inducibility of cerebellar LTD. (*A*) In WT cerebellum, GluD2 maintains low levels of phosphorylation at Y876 of the GluA2 subunit of AMPA receptors through PTPMEG that binds to the C terminus. LTD-inducing stimuli further dephosphorylate Y876 by unknown mechanisms, including activation of PTPMEG by conformational changes of GluD2 and inactivation of SFKs. Y876 dephosphorylation allows S880 phosphorylation by PKC, leading to the replacement of anchoring proteins from glutamate receptor interacting protein (GRIP) to PICK1 and allowing AMPA receptor endocytosis during LTD. (*B*) In *GluD2*-null and *PTPMEG*-null Purkinje cells, high basal-state phosphorylation at Y876 prevents subsequent phosphorylation at S880 of GluA2 during LTD-inducing stimulus, thus inhibiting GluA2 endocytosis and LTD.

remains unclear whether Y876 in GluA2 serves as a substrate for STEP. In addition, little STEP mRNA is expressed in the cerebellum (42). In this study, we identified GluA2 as a substrate for PTPMEG with a substrate trap mutant of PTPMEG (Fig. 7*A*). An in vitro dephosphorylation assay with pep-3pY (Fig. 7*B*) and GluA2-expressing cells (Fig. 7*C*) confirmed that Y876 in GluA2 was a substrate for PTPMEG. In addition, we identified VCP as a substrate for PTPMEG with a substrate trap assay. PTPMEG has also been shown to interact with and dephosphorylate the T-cell receptor-ζ (43). Therefore, in addition to GluA2, other proteins could be dephosphorylated by PTPMEG in Purkinje cells. Because many synaptic proteins, such as β-catenin, *N*-cadherin, and ephrinB, are tyrosine-phosphorylated and regulate various aspects of synaptic functions, future studies are warranted to further identify substrates of PTPMEG.

An important question remains as to how increased neuronal activity decreases Y876 dephosphorylation (Fig. 2*A*). This dephosphorylation could be achieved independent of GluD2. For example, SFKs are down-regulated during LTD (31), thereby decreasing Y876 phosphorylation independently of GluD2. However, GluD2 may mediate not only basal but also activity-dependent Y876 dephosphorylation through the interaction with PTPMEG, because in *GluD2*-null (Fig. 2*B*) or *PTPMEG*-null (Fig. 5*D*) cerebellum, K-glu did not decrease Y876 phosphorylation. In the hippocampus, STEP is rapidly translated in response to mGluR activation (41). Because protein translation has been suggested to play a role in cerebellar LTD (44), PTPMEG may be one of the molecules with translation that is induced by mGluR. PTPMEG has also shown to be activated four- to eightfold on calpain-induced cleavage (45), which could be triggered by increases in intracellular Ca^{2+} concentrations during LTD induction. Finally, the activities of protein phosphatases have been reported to be regulated by their oligomerization status (46). Because Cbln1, which is released from granule cells, causes GluD2 clustering by binding to the N-terminal domain of GluD2 (47), it may activate PTPMEG by aggregating PTPMEG at PF synapses in Purkinje cells. D-Ser, which is released from Bergmann glia in an activity-dependent manner in immature cerebellum, binds to the ligand-binding domain of GluD2 and facilitates AMPA receptor endocytosis and LTD (48). Thus, the conformational changes that are induced by the binding of D-Ser may also regulate PTPMEG activities. Future studies are warranted to clarify whether and how GluD2-PTPMEG signaling is regulated to balance tyrosine phosphorylation and dephosphorylation levels of GluA2 for the fine tuning of AMPA receptor endocytosis.

Materials and Methods

Electrophysiology. Whole-cell patch-clamp recordings were made from visually identified Purkinje cells. Parasagittal cerebellar slices (200-μm thick) were prepared from WT, *GluD2*-null, or *PTPMEG*-null mice on P21–P35 as described previously (48). All procedures relating to the care and treatment of animals were performed in accordance with National Institutes of Health guidelines and permitted by Keio University Experimental Animal Committee.

Virus Vector Constructs and in Vivo Microinjection. For transduction of mutant transgenes into cerebellar Purkinje cells, we used a modified Sindbis virus

vector (Invitrogen), which contained an additional subgenomic promoter and GFP (3, 49). When we transduced GluA2, we used GluA2, which carried glutamine (Q) in its Q/R RNA editing site to increase cell surface expression.

Mass Spectrometric Analysis. A synthetic phosphorylated GluA2 C-terminal peptide, pep-3pY, was used as a substrate. GST-PTP^{WT}, its mutants (D820A and C852S), and GST were prebound to glutathione Sepharose beads (GE Healthcare). Dephosphorylation reaction of pep-3pY (20 pmol) was performed for 30 min at 30 °C in the buffer containing 25 mM Hepes (pH 7.35), 5 mM EDTA, and 10 mM DTT by adding 2 μg each GST protein. GluA2 peptides in the supernatant were purified and concentrated using StageTips (Empore extraction disk; 3M) and labeled with four iTRAQ reagents (Applied Biosystems/MDS Sciex). iTRAQ-labeled GluA2 peptides were mixed and concentrated by vacuum evaporation, and they were subjected to mass spectrometric analysis using a 4800 MALDI-TOF-TOF Analyzer (Applied Biosystems/MDS). Peak areas for each iTRAQ signature were obtained by using ProteinPilot. For quantitative comparison, the data were normalized by the peak area of GST-treated sample.

More details are in *SI Materials and Methods*.

Statistical Analysis. The results were described as means ± SEM. Statistical significance was defined as $P < 0.05$. When we compare the two groups, Mann–Whitney *U* test was used. We performed Student *t* test in the case of comparing the normalized values to the control (=1). To compare multiple groups, one-way ANOVA followed by Bonferroni posthoc test was performed.

ACKNOWLEDGMENTS. We thank Dr. R. L. Huganir and Dr. T. Hayashi for the antiphosphoY876 GluA2 antibody, Dr. M. Watanabe for the anti-mGluR1α antibody, and Dr. M. Mishina for the *GluD2*-null mouse. We also thank J. Motohashi and S. Narumi for their technical assistance. This work was supported by a Grant-in-Aid for the Ministry of Education, Culture, Sports, Science and Technology of Japan (to K.K., W.K., and M.Y.), the Keio Gijuku Academic Development Funds (K.K. and W.K.), the Keio University Medical Science Fund, Research Grants for Life Science and Medicine (to K.K. and W.K.), the Naito Foundation (W.K.), the Inamori Foundation (W.K.), the Nakajima Foundation (W.K.), the Takeda Science Foundation (W.K. and M.Y.), the Precursory Research for Embryonic Science and Technology (PRESTO) program from the Japan Science and Technology Agency (JST) (S.M.), and the Core Research for Evolutional Science and Technology (CREST) from the JST (M.Y.).

1. Ito M (2002) The molecular organization of cerebellar long-term depression. *Nat Rev Neurosci* 3(11):896–902.
2. Kashiwabuchi N, et al. (1995) Impairment of motor coordination, Purkinje cell synapse formation, and cerebellar long-term depression in GluR delta 2 mutant mice. *Cell* 81(2):245–252.
3. Kohda K, et al. (2007) The extreme C-terminus of GluRdelta2 is essential for induction of long-term depression in cerebellar slices. *Eur J Neurosci* 25(5):1357–1362.
4. Kakegawa W, et al. (2008) Differential regulation of synaptic plasticity and cerebellar motor learning by the C-terminal PDZ-binding motif of GluRdelta2. *J Neurosci* 28(6): 1460–1468.
5. Yuzaki M (2009) New (but old) molecules regulating synapse integrity and plasticity: Cbln1 and the delta2 glutamate receptor. *Neuroscience* 162(3):633–643.
6. Man HY, et al. (2000) Regulation of AMPA receptor-mediated synaptic transmission by clathrin-dependent receptor internalization. *Neuron* 25(3):649–662.
7. Seidenman KJ, Steinberg JP, Huganir R, Malinow R (2003) Glutamate receptor subunit 2 Serine 880 phosphorylation modulates synaptic transmission and mediates plasticity in CA1 pyramidal cells. *J Neurosci* 23(27):9220–9228.
8. Matsuda S, Launey T, Mikawa S, Hirai H (2000) Disruption of AMPA receptor GluR2 clusters following long-term depression induction in cerebellar Purkinje neurons. *EMBO J* 19(12):2765–2774.
9. Wang YT, Linden DJ (2000) Expression of cerebellar long-term depression requires postsynaptic clathrin-mediated endocytosis. *Neuron* 25(3):635–647.
10. Chung HJ, Steinberg JP, Huganir RL, Linden DJ (2003) Requirement of AMPA receptor GluR2 phosphorylation for cerebellar long-term depression. *Science* 300(5626): 1751–1755.
11. Ahmadian G, et al. (2004) Tyrosine phosphorylation of GluR2 is required for insulin-stimulated AMPA receptor endocytosis and LTD. *EMBO J* 23(5):1040–1050.
12. Moult PR, et al. (2006) Tyrosine phosphatases regulate AMPA receptor trafficking during metabotropic glutamate receptor-mediated long-term depression. *J Neurosci* 26(9):2544–2554.
13. Gladding CM, et al. (2009) Tyrosine dephosphorylation regulates AMPAR internalisation in mGluR-LTD. *Mol Cell Neurosci* 40(2):267–279.
14. Scholz R, et al. (2010) AMPA receptor signaling through BRAG2 and Arf6 critical for long-term synaptic depression. *Neuron* 66(5):768–780.
15. Hironaka K, Umemori H, Tezuka T, Mishina M, Yamamoto T (2000) The protein-tyrosine phosphatase PTPMEG interacts with glutamate receptor delta 2 and epsilon subunits. *J Biol Chem* 275(21):16167–16173.
16. Hayashi T, Huganir RL (2004) Tyrosine phosphorylation and regulation of the AMPA receptor by SRC family tyrosine kinases. *J Neurosci* 24(27):6152–6160.
17. Canepari M, Ogden D (2003) Evidence for protein tyrosine phosphatase, tyrosine kinase, and G-protein regulation of the parallel fiber metabotropic slow EPSC of rat cerebellar Purkinje neurons. *J Neurosci* 23(10):4066–4071.
18. Kim SJ, et al. (2003) Activation of the TRPC1 cation channel by metabotropic glutamate receptor mGluR1. *Nature* 426(6964):285–291.
19. Hartmann J, et al. (2008) TRPC3 channels are required for synaptic transmission and motor coordination. *Neuron* 59(3):392–398.
20. Jeromin A, Huganir RL, Linden DJ (1996) Suppression of the glutamate receptor delta 2 subunit produces a specific impairment in cerebellar long-term depression. *J Neurophysiol* 76(5):3578–3583.
21. Tanaka K, Augustine GJ (2008) A positive feedback signal transduction loop determines timing of cerebellar long-term depression. *Neuron* 59(4):608–620.
22. Huang CC, Hsu KS (2006) Sustained activation of metabotropic glutamate receptor 5 and protein tyrosine phosphatases mediate the expression of (S)-3,5-dihydroxyphenylglycine-induced long-term depression in the hippocampal CA1 region. *J Neurochem* 96(1): 179–194.
23. Yu SY, Wu DC, Liu L, Ge Y, Wang YT (2008) Role of AMPA receptor trafficking in NMDA receptor-dependent synaptic plasticity in the rat lateral amygdala. *J Neurochem* 106(2):889–899.
24. Brebner K, et al. (2005) Nucleus accumbens long-term depression and the expression of behavioral sensitization. *Science* 310(5752):1340–1343.
25. Kina S, et al. (2007) Involvement of protein-tyrosine phosphatase PTPMEG in motor learning and cerebellar long-term depression. *Eur J Neurosci* 26(8):2269–2278.
26. Tiganis T, Bennett AM (2007) Protein tyrosine phosphatase function: The substrate perspective. *Biochem J* 402(1):1–15.
27. Zhang SH, Liu J, Kobayashi R, Tonks NK (1999) Identification of the cell cycle regulator VCP (p97/CDC48) as a substrate of the band 4.1-related protein-tyrosine phosphatase PTPH1. *J Biol Chem* 274(25):17806–17812.
28. Yuzaki M, Cerebellar LTD vs. motor learning-Lessons learned from studying GluD2. *Neural Netw*, in press.
29. Boxall AR, Lancaster B, Garthwaite J (1996) Tyrosine kinase is required for long-term depression in the cerebellum. *Neuron* 16(4):805–813.
30. Hartell NA (2001) Receptors, second messengers and protein kinases required for heterosynaptic cerebellar long-term depression. *Neuropharmacology* 40(1):148–161.
31. Tsuruno S, Kawaguchi SY, Hirano T (2008) Src-family protein tyrosine kinase negatively regulates cerebellar long-term depression. *Neurosci Res* 61(3):329–332.
32. Lüscher C, Huber KM (2010) Group 1 mGluR-dependent synaptic long-term depression: Mechanisms and implications for circuitry and disease. *Neuron* 65(4):445–459.
33. Gladding CM, Fitzjohn SM, Molnár E (2009) Metabotropic glutamate receptor-mediated long-term depression: Molecular mechanisms. *Pharmacol Rev* 61(4):395–412.
34. Liu YF, et al. (2004) Serine phosphorylation proximal to its phosphotyrosine binding domain inhibits insulin receptor substrate 1 function and promotes insulin resistance. *Mol Cell Biol* 24(21):9668–9681.
35. Sanz-Clemente A, Matta JA, Isaac JT, Roche KW (2010) Casein kinase 2 regulates the NR2 subunit composition of synaptic NMDA receptors. *Neuron* 67(6):984–996.
36. Unoki T, et al. (2012) NMDA receptor-mediated PIP5K activation to produce PI(4,5)P_2 is essential for AMPA receptor endocytosis during LTD. *Neuron* 73(1):135–148.
37. Lomeli H, et al. (1993) The rat delta-1 and delta-2 subunits extend the excitatory amino acid receptor family. *FEBS Lett* 315(3):318–322.
38. Kim CH, Chung HJ, Lee HK, Huganir RL (2001) Interaction of the AMPA receptor subunit GluR2/3 with PDZ domains regulates hippocampal long-term depression. *Proc Natl Acad Sci USA* 98(20):11725–11730.
39. Takeuchi T, et al. (2008) Enhancement of both long-term depression induction and optokinetic response adaptation in mice lacking delphilin. *PLoS ONE* 3(5):e2297.
40. Miyagi Y, et al. (2002) Delphilin: A novel PDZ and formin homology domain-containing protein that synaptically colocalizes and interacts with glutamate receptor delta 2 subunit. *J Neurosci* 22(3):803–814.
41. Zhang Y, et al. (2008) The tyrosine phosphatase STEP mediates AMPA receptor endocytosis after metabotropic glutamate receptor stimulation. *J Neurosci* 28(42): 10561–10566.
42. Lombroso PJ, Murdoch G, Lerner M (1991) Molecular characterization of a protein-tyrosine-phosphatase enriched in striatum. *Proc Natl Acad Sci USA* 88(16):7242–7246.
43. Young JA, et al. (2008) The protein tyrosine phosphatase PTPN4/PTP-MEG1, an enzyme capable of dephosphorylating the TCR ITAMs and regulating NF-kappaB, is dispensable for T cell development and/or T cell effector functions. *Mol Immunol* 45(14):3756–3766.
44. Linden DJ (1996) A protein synthesis-dependent late phase of cerebellar long-term depression. *Neuron* 17(3):483–490.
45. Gu M, Majerus PW (1996) The properties of the protein tyrosine phosphatase PTPMEG. *J Biol Chem* 271(44):27751–27759.
46. Coles CH, et al. (2011) Proteoglycan-specific molecular switch for RPTPσ clustering and neuronal extension. *Science* 332(6028):484–488.
47. Matsuda K, et al. (2010) Cbln1 is a ligand for an orphan glutamate receptor delta2, a bidirectional synapse organizer. *Science* 328(5976):363–368.
48. Kakegawa W, et al. (2011) D-serine regulates cerebellar LTD and motor coordination through the δ2 glutamate receptor. *Nat Neurosci* 14(5):603–611.
49. Kakegawa W, Kohda K, Yuzaki M (2007) The delta2 'ionotropic' glutamate receptor functions as a non-ionotropic receptor to control cerebellar synaptic plasticity. *J Physiol* 584(Pt 1):89–96.